

Thermodynamics and Phase Relationships of the Ternary Lanthanum-Uranium-Oxygen System

E. STADLBAUER, U. WICHMANN, U. LOTT, AND C. KELLER

Institut für Radiochemie, Kernforschungszentrum Karlsruhe, Postfach 3640, Germany

Received October 29, 1973

In the selected regions $\text{La}:(\text{La} + \text{U}) = 0.05$ and $\text{O}:(\text{La} + \text{U}) = 2.00$ of the ternary system lanthanum-uranium-oxygen emf measurements on solid state galvanic cells, coulometric titrations, and X-ray diffraction techniques were used to obtain phase boundaries and thermodynamic data in the temperature range from 600 to 1000°C. For the first time order \rightleftharpoons disorder transformations of $\text{La}_{1-y}\text{U}_y\text{O}_{2+x}$ up to 15 mole % lanthanum are reported. The transformation temperature is 1415°K for $\text{UO}_{2.23}$; 1397°K for $\text{La}_{0.05}\text{U}_{0.95}\text{O}_{2.23}$, and 1449°K for $\text{La}_{0.15}\text{U}_{0.85}\text{O}_{2.23}$. The vibrational entropy component of excess oxygen in $\text{M}_{1-y}\text{U}_y\text{O}_{2+x}$ is estimated.

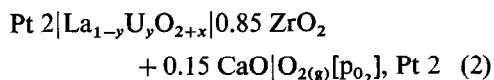
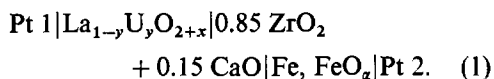
1. Introduction

Phase relations in the lanthanum-uranium-oxygen system have been investigated under various experimental conditions (1-7). In this laboratory Diehl and Keller clarified the phase relationships in the UO_2 - UO_3 - $\text{LaO}_{1.5}$ region at 1250°C using X-ray diffraction techniques (8). They found five single phase regions: β - U_3O_8 , $\text{LaO}_{1.5}$, a fluorite phase F , a rhombohedral phase R_I , and a rhombohedral phase R_{II} . Their results are summarized in Fig. 1. The phase boundaries outside the UO_2 - UO_3 - $\text{LaO}_{1.5}$ region are defined as a result of topological considerations. The numbers indicate the phases in equilibrium and the meaning of the dashed and solid lines are explained in the diagram.

X-ray diffraction techniques and emf measurements using high-temperature galvanic cells (9, 10) were used in our investigation to determine order \rightleftharpoons disorder transformations and thermodynamic data of the UO_2 - UO_3 - $\text{LaO}_{1.5}$ system. The results were compared with those of the uranium-oxygen system (12).

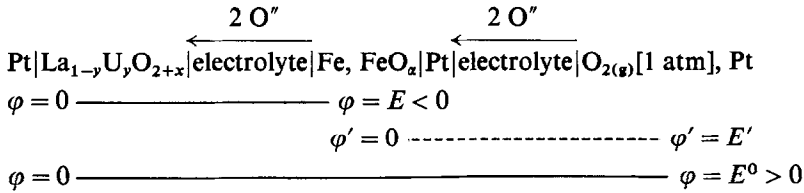
2. Theory

For a better understanding of the experimental procedure a few theoretical aspects will be briefly reviewed. The basic tools in investigating the subject were galvanic cells with pure anionic conductivity of the electrolyte ($0.85 \text{ ZrO}_2 + 0.15 \text{ CaO}$):



$$(0.5 \leq y \leq 1 \text{ and } x < 0.35).$$

In each cell there is a lower limit of the emf measurements of about 600°C given by the decrease in the mobility of the oxygen ion vacancies with decreasing temperature. The relation between the standard emf E^0 (cell II) and the emf E (cell I) with an iron-wustite reference electrode is evidenced by the following arrangement:



Since $E^0 = E + E'$ and $E' = -(1/2F)\Delta_f G_{\text{FeO}_\alpha}^0$ we obtain $E^0 = E - (1/2F)\Delta_f G_{\text{FeO}_\alpha}^0$.

In these equations φ is the galvanic potential and $\Delta_f G_{\text{FeO}_\alpha}^0$ the standard molar free enthalpy of formation of FeO (α approximately = 1). The measured emf values and their temperature coefficients give the standard molar free enthalpy change ΔG^0 , the standard molar enthalpy change ΔH^0 , and the standard molar entropy change ΔS^0 of reaction. The standard equations read:

$$\begin{aligned}
 \Delta G^0 &= -|z|FE^0; \\
 \Delta S^0 &= -(\partial\Delta G^0/\partial T)_P = |z|F(\partial E^0/\partial T)_P; \\
 \Delta H^0 &= -|z|F[E^0 - T(\partial E^0/\partial T)_P]; \text{ and also} \\
 p_{\text{O}_2} &= p_{\text{O}_2}^0 \exp \frac{\Delta G^0}{RT};
 \end{aligned}$$

where z is the number of electrons in the given electrode reaction, F the Faraday constant, p the partial pressure, R the ideal gas constant, and P the number of phases. As described in more detail in previous reports (7, 11) the experimental result $\partial E/\partial x = 0$ indicates a two-phase region and $\partial E/\partial x \neq 0$ a single-phase region.

3. Experimental

The specimens $\text{La}_{1-y}\text{U}_y\text{O}_{2+x}$ were prepared by mixing weighted amounts of UO_2 , U_3O_8 , and La_2O_3 . The mixtures were filled into platinum crucibles and then heated at 1000°C or 1250°C for about two months in evacuated quartz tubes. Next they were quenched in

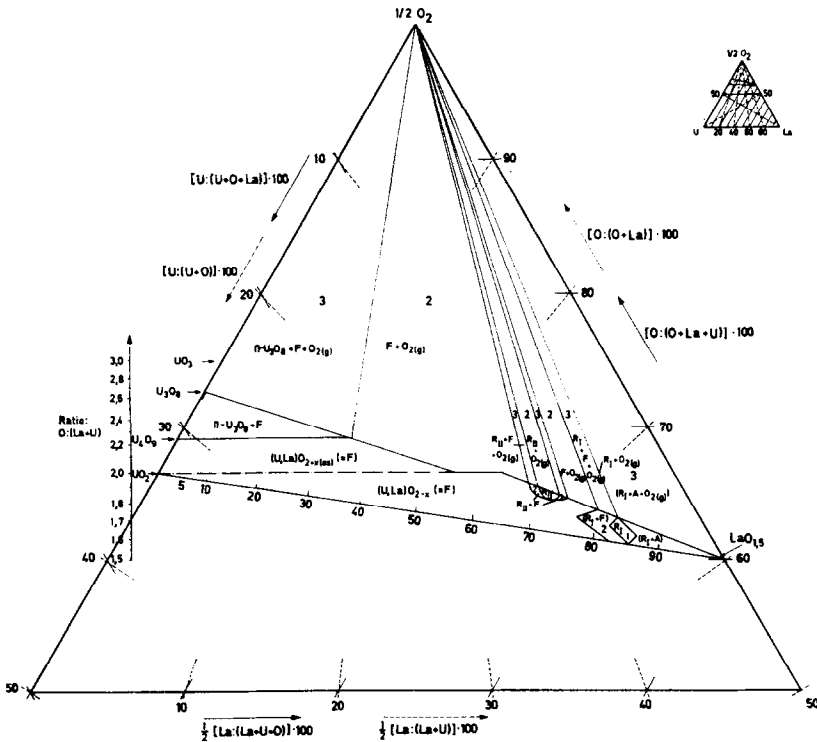


Fig. 1. Phase relations in the system La-U-O at 1250°C .

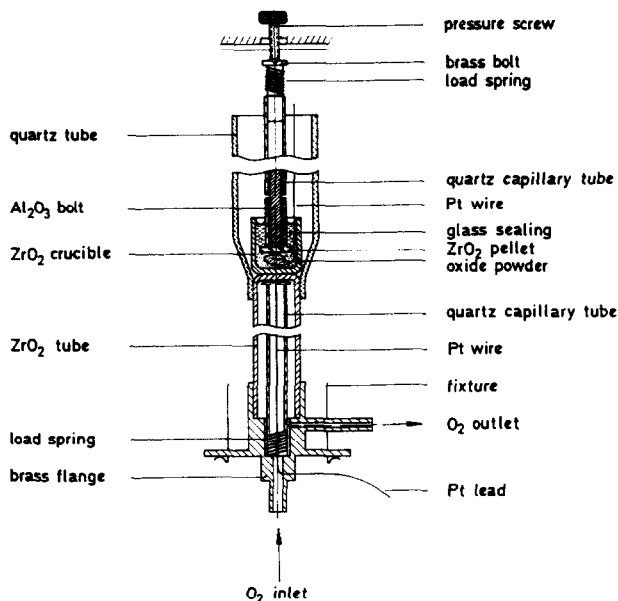


FIG. 2. Design of the galvanic cell II with a standard oxygen reference electrode.

liquid nitrogen and analysed by cerimetric titration (8); the accuracy of x is ± 0.02 . The lattice constants were determined by X-ray diffraction.

The design of the galvanic cell II, provided with a standard oxygen reference electrode, is shown in Fig. 2, whereas in cell I the gaseous standard oxygen reference electrode was substituted by a solid iron-wustite electrode. About 100–200 mg of oxide powder $\text{La}_{1-y}\text{U}_y\text{O}_{2+x}$ were put into a small doped ZrO_2 crucible which was used as a solid state electrolyte. The oxide powder was covered with a ZrO_2 pellet, and a quartz capillary tube was pressed onto this pellet using a load spring. Thus a close contact is maintained to the solid state electrolyte at high temperatures when the oxide sinters. The oxide powder was isolated from the environment by filling up the doped ZrO_2 crucible with AR-glass (AR-glass produces a liquid gasket at high temperatures).

The electronic contact was provided by a Pt-wire which ran through the glass gasket and the ZrO_2 pellet to the oxide powder. The whole half cell was pressed onto the standard oxygen electrode consisting of a long

tube of doped ZrO_2 . The inside bottom of this tube was platinized. In addition, a quartz capillary tube was pressed onto the inner side of the tube using a load spring. This capillary carried the electronic contacts and was used to flow oxygen into the tube. Thus, at the Pt/electrolyte phase boundary a slow flow of oxygen (1 atm) could be maintained. The other end of the long ZrO_2 tube was sealed to a brass flange equipped with an oxygen inlet and outlet as well as Pt-contacts. The two half cells were brought into contact by spring pressure. The apparatus was placed in another quartz tube closed by ground joints on both sides. For temperatures higher than 1200°C quartz was replaced by ceramic materials.

At the beginning of each measurement the whole system was flushed with nitrogen. Nitrogen was purified by passing it over oxidized BTS-catalyst, various molecular sieves, and a reduced BTS-catalyst ($p_{\text{O}_2} \sim 10^{-8}$ atm). Next, the cell was heated up quickly to 1000°C to melt the AR-glass. During each experiment, the temperature and emf were continuously recorded, and readings were not made until stable emf values have

been obtained. The temperature was lowered or increased by increments of 50–100°C, and equilibration required 2–24 hr.

A certain amount of oxygen was electrically transferred into or out of a half cell by coulometric titration (12). To change a given composition of $\text{La}_{1-y}\text{U}_y\text{O}_{2+x}$ from x to $x + \Delta x$ the charge $\Delta Q = I\Delta t = (m/M)\Delta x 2F$ is required, where m is the mass, M the molecular mass of the substance $\text{La}_{1-y}\text{U}_y\text{O}_{2+x}$, I the current, Δt the time interval, $I \leq 0.1$ mA and $\Delta x \leq 0.01$. Polarization was smaller in cell I than in cell II. This is probably due to the fact that in the standard oxygen electrode there is no decrease in oxygen. Generally, after a period of 12 hr, a constant emf value was reached. The reproducibility was ± 5 mV. All calculations were made on a "Wang 700 B," using a computer program.

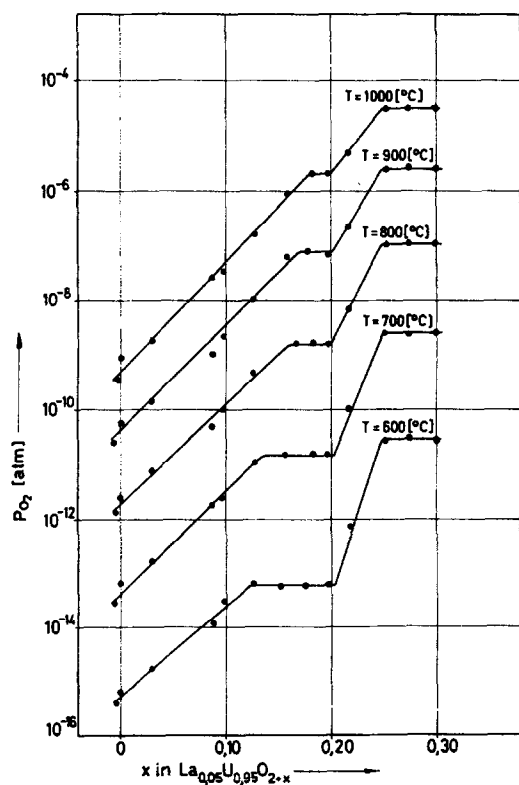


FIG. 3. Oxygen partial pressure (p_{O_2}) for compositions $\text{La}_{0.05}\text{U}_{0.95}\text{O}_{2+x}$ as a function of x and temperature ($-0.02 \leq x \leq 0.35$).

4. Results and Discussion of emf Measurements

4.1. The region with a Ratio $\text{La}/(\text{La} + \text{U}) = 0.05$ and $\text{La}_{1-y}\text{U}_y\text{O}_{2.23}$

In Fig. 3 the oxygen partial pressure (p_{O_2}) is plotted as a function of the composition x in $\text{La}_{0.05}\text{U}_{0.95}\text{O}_{2+x}$ for different temperatures. In two regions the oxygen partial pressure remains unchanged with composition, an indication of a two-phase region. Also, there are two single-phase regions in which the oxygen partial pressure value varies with a small change of x in $\text{La}_{0.05}\text{U}_{0.95}\text{O}_{2+x}$.

Obviously, at low lanthanum oxide content, the oxygen potential in the uranium oxide-lanthanum oxide system shows a behaviour similar to the binary uranium oxide system (12). The appearance of these single and two-phase regions in the investigated temperature range is due to a solubility of lanthanum oxide in the fluorite phase of the nonstoichiometric uranium dioxide. Specimens with the same mean valency of uranium, e.g., $\text{UO}_{2+x'}$ and $\text{La}_{0.05}\text{U}_{0.95}\text{O}_{2+x}$ (the latter composed of $\text{UO}_{2+x'}$ and 5 mole% lanthanum oxide) were prepared under identical conditions. It is interesting to compare the lattice parameter of the specimens $\text{UO}_{2+x'}$ with that of the corresponding $\text{La}_{0.05}\text{U}_{0.95}\text{O}_{2+x}$. It was observed that the solubility of lanthanum oxide in the fluorite phase of nonstoichiometric

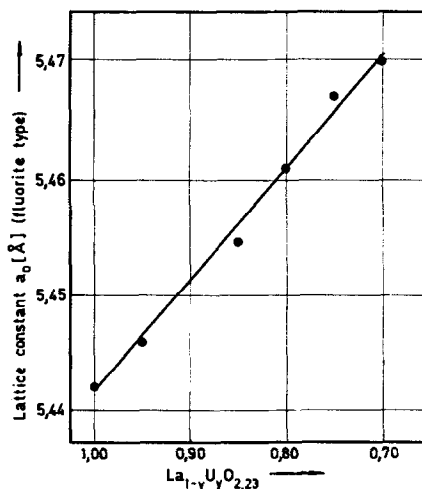


FIG. 4. Lattice constant of $\text{La}_{1-y}\text{U}_y\text{O}_{2.23}$ as a function of y ($T = 25^\circ\text{C}$), quenched samples, prepared at 1000°C .

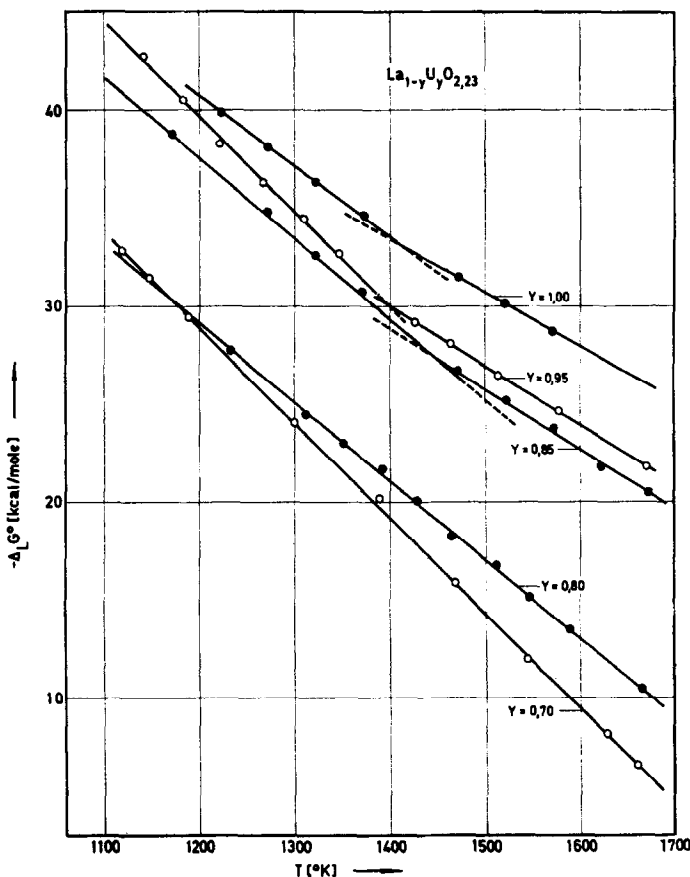


FIG. 5. Standard molar free enthalpy change $\Delta_L G^\circ$ of solution of the specimens $\text{La}_{1-y}\text{U}_y\text{O}_{2.23}$ as a function of temperature ($0.7 \leq y \leq 1$).

uranium dioxide caused an increase in the lattice constant as expected. In addition, X-ray diffractions of mixtures from $\text{La}_{0.05}\text{U}_{0.95}\text{O}_{2.21}$ up to $\text{La}_{0.05}\text{U}_{0.95}\text{O}_{2.25}$ showed strong lines of the dioxide lattice and additional reflexes—so-called superstructural lines—at high angles of the ordered structure of the U_4O_9 type. This latter observation is evidence that the ordered single-phase region of U_4O_{9-x} is preserved when small amounts of lanthanum oxide are incorporated into its lattice. The increase of the lattice constant of $\text{La}_{1-y}\text{U}_y\text{O}_{2.23}$ with increasing y (see Fig. 4) demonstrates the solubility of lanthanum oxide in the U_4O_{9-x} -phase, but superstructural lines of decreasing intensity were seen only up to $\text{La}_{0.15}\text{U}_{0.85}\text{O}_{2.23}$.

To decide in which regions an ordered or

disordered crystal structure was produced, we investigated the behaviour of $\Delta_L G^\circ$ of the specimens $\text{La}_{1-y}\text{U}_y\text{O}_{2.23}$ as a function of temperature. Figure 5 shows that in the case of $\text{UO}_{2.23}$ the order \rightleftharpoons disorder transformation to UO_{2-x} causes a definite break in the $\Delta_L G^\circ$ -curve at 1415°K. This temperature is in agreement with literature data on the transformation of ordered U_4O_{9-x} into disordered $\text{UO}_{2.23}$ (13). At higher temperatures the state of order is disturbed. The transformation temperature of the order \rightleftharpoons disorder transformation is 1397°K for $\text{La}_{0.05}\text{U}_{0.95}\text{O}_{2.23}$ and 1449°K for $\text{La}_{0.15}\text{U}_{0.85}\text{O}_{2.23}$.

The $\Delta_L G^\circ$ -function for $\text{La}_{0.2}\text{U}_{0.8}\text{O}_{2.23}$ and $\text{La}_{0.3}\text{U}_{0.7}\text{O}_{2.23}$ shows a straight line indicating that also at low temperatures the disordered phase is conserved.

The thermodynamic equations for $\text{La}_{1-y}\text{U}_y\text{O}_{2.23}$ read

For $y = 1.00$:

$$1200 < T \leq 1415^\circ\text{K} \quad \Delta_L G^\circ$$

$$= (-83.2 \pm 0.3) \frac{\text{kcal}}{\text{mole}} + (35.4 \pm 0.2) \frac{\text{cal}}{\text{mole deg}} T.$$

$$1415 \leq T < 1580^\circ\text{K} \quad \Delta_L G^\circ$$

$$= (-72.4 \pm 0.5) \frac{\text{kcal}}{\text{mole}} + (27.8 \pm 0.3) \frac{\text{cal}}{\text{mole deg}} T.$$

$$\Delta(\Delta_L G^\circ) = (-10.8 \pm 0.6) \frac{\text{kcal}}{\text{mole}} \\ + (7.6 \pm 0.4) \frac{\text{cal}}{\text{mole deg}} T.$$

$$\Delta(\Delta_L G^\circ) = 0 \text{ if } T = 1415^\circ\text{K}.$$

For $y = 0.95$;

$$1045 < T \leq 1397^\circ\text{K} \quad \Delta_L G^\circ$$

$$= (-98.2 \pm 1.0) \frac{\text{kcal}}{\text{mole}} + (48.7 \pm 0.8) \frac{\text{cal}}{\text{mole deg}} T.$$

$$1397 \leq T < 1680^\circ\text{K} \quad \Delta_L G^\circ$$

$$= (-73.0 \pm 0.3) \frac{\text{kcal}}{\text{mole}} + (30.7 \pm 0.2) \frac{\text{cal}}{\text{mole deg}} T.$$

$$\Delta(\Delta_L G^\circ) = (-25.2 \pm 1.1) \frac{\text{kcal}}{\text{mole}} \\ + (18.0 \pm 0.9) \frac{\text{cal}}{\text{mole deg}} T.$$

$$\Delta(\Delta_L G^\circ) = 0 \text{ if } T = 1397^\circ\text{K}.$$

For $y = 0.85$;

$$1170 < T \leq 1449^\circ\text{K} \quad \Delta_L G^\circ$$

$$= (-87.0 \pm 0.5) \frac{\text{kcal}}{\text{mole}} + (41.0 \pm 0.4) \frac{\text{cal}}{\text{mole deg}} T.$$

$$1449 \leq T < 1680^\circ\text{K} \quad \Delta_L G^\circ$$

$$= (-73.9 \pm 1.3) \frac{\text{kcal}}{\text{mole}} + (32.0 \pm 0.8) \frac{\text{cal}}{\text{mole deg}} T.$$

$$\Delta(\Delta_L G^\circ) = (-13.1 \pm 1.4) \frac{\text{kcal}}{\text{mole}} \\ + (9.0 \pm 0.9) \frac{\text{cal}}{\text{mole deg}} T.$$

$$\Delta(\Delta_L G^\circ) = 0 \text{ if } T = 1449^\circ\text{K}.$$

For $y = 0.80$;

$$1060 \leq T \leq 1670^\circ\text{K} \quad \Delta_L G^\circ$$

$$= (-78.6 \pm 0.7) \frac{\text{kcal}}{\text{mole}} + (41.0 \pm 0.5) \frac{\text{cal}}{\text{mole deg}} T$$

For $y = 0.70$;

$$1060 \leq T \leq 1630^\circ\text{K} \quad \Delta_L G^\circ$$

$$= (-88.1 \pm 1.1) \frac{\text{kcal}}{\text{mole}} + (49.1 \pm 0.8) \frac{\text{cal}}{\text{mole deg}} T.$$

These results demonstrate that uranium atoms in the U_4O_{9-x} -superstructure may be replaced by trivalent metal atoms. The limit is found between 15 to 20 mole% lanthanum. Until now it only has been shown that tetravalent uranium atoms can be substituted by Th, Np, or Pu to yield, e.g., $\text{Th}_2\text{U}_2\text{O}_9$ (14).

4.2. The Region with a Ratio $O:(\text{La} + \text{U}) = 2.00$

In Fig. 6 the emf is plotted versus the temperature. At constant temperature there is no change in the emf value for compositions from $\text{La}_{0.50}\text{U}_{0.50}\text{O}_{1.98}$ up to $\text{La}_{0.50}\text{U}_{0.50}\text{O}_{2.03}$. This indicates that $\text{La}_{0.50}\text{U}_{0.50}\text{O}_{2.00}$ is a point in a two-phase region. Some additional information was obtained from X-ray investigations (Figs. 7a and b). At 1250°C single-phase $\text{La}_{0.50}\text{U}_{0.50}\text{O}_{2.00}$ crystallizes in the fluorite structure (Fig. 7a). With decreasing temperature, additional lines occur at $1130 \pm 20^\circ\text{C}$, indicating that here the specimen of the formal composition $\text{La}_{0.50}\text{U}_{0.50}\text{O}_{2.00}$ belongs to a two-phase region (Fig. 7b). In the diagram the additional lines are indexed rhombohedrally according to investigations by Rüdorff et al. in the system $\text{U}_2\text{O}_5\text{-La}_2\text{O}_3$ (6). The phase transformation at $1130 \pm 20^\circ\text{C}$ is reversible and takes place quickly. The width of the bi-phasic region is from $\text{La}_{0.50}\text{U}_{0.50}\text{O}_{1.98}$ up to $\text{La}_{0.50}\text{U}_{0.50}\text{O}_{2.03}$, and the composition $\text{La}_{0.47}\text{U}_{0.53}\text{O}_{2.00}$ has a single-phase structure in the temperature region investigated.

The thermodynamic data are given in Fig. 8. The standard molar free enthalpy change $\Delta_L G^\circ$ of solution is a linear function of the temperature. At a constant temperature it increases with increasing lanthanum content. Phase transformation causes a definite break.

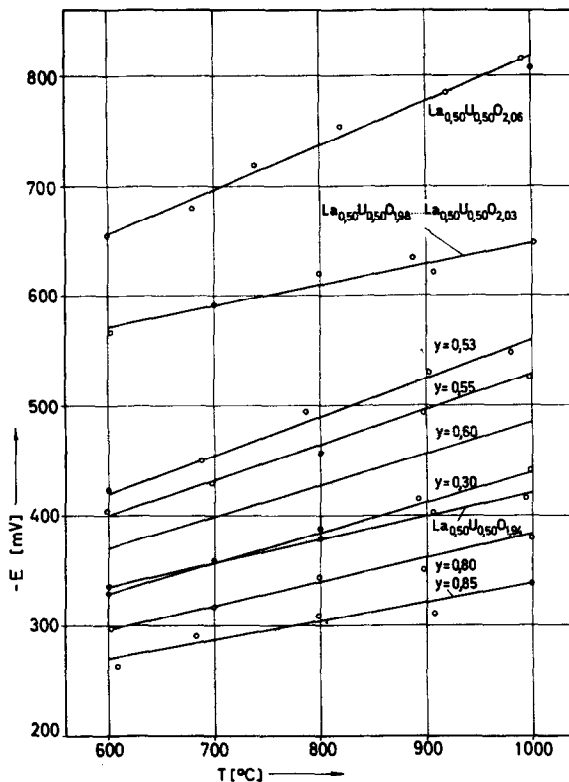


FIG. 6. Emf for some selected compositions as a function of temperature.

Whereas $\Delta_L S^0$ decreases with increasing lanthanum content, $\Delta_L H^0$ increases with increasing lanthanum content up to 20 mole % lanthanum and then remains nearly constant.

Comparison of the thermodynamic data of $La_{1-y}U_yO_{2.00}$ with that of $UO_{2.00}$ (Fig. 8) shows that the increasing substitution of uranium ions by lanthanum ions causes changes in the thermodynamic functions. $\Delta_L G^0$ increases, while $\Delta_L S^0$ and $\Delta_L H^0$ decrease. The change in the thermodynamic functions is paralleled by an increase in the lattice constant (Fig. 9).

4.3. Estimate of Vibrational Entropy of Interstitial Oxygen in $M_{1-y}U_yO_{2+x}$

Mainly two different methods are described in the literature for computation of the vibrational entropy of oxygen in a nonstoichiometric solid state compound: First the calculation of the entropy on the basis of the development of a generalized partition function for a

canonical ensemble of defects (15, 16), and second, the calculation of the configurational entropy using an ionic picture and assigning to the vibrational entropy the differences between the solution entropy based on experimental data and the corresponding values from the ionic model (17). Following the latter treatment, developed by Aronson we describe the solution of oxygen in the nonstoichiometric $M_{1-y}U_yO_{2+x}$ (M is a metal ion in a given state) by the following basic equations:

$$O_2 = 2O'' + 4|e|\cdot \tag{1}$$

$$4U|U|^{4+} + 4|e|\cdot = 4U|U|^{5+} \tag{2}$$

Schottky's Minimal-Symbolic has been used, according to which $U|U|^{4+}$ is an uranium-IV-cation in a lattice position, $U|U|^{5+}$ is an uranium-V-cation in a lattice position, $|e|\cdot$ is a defect electron, and O'' is an oxygen ion in an interstitial position. In the following equations N indicates the number of speci-

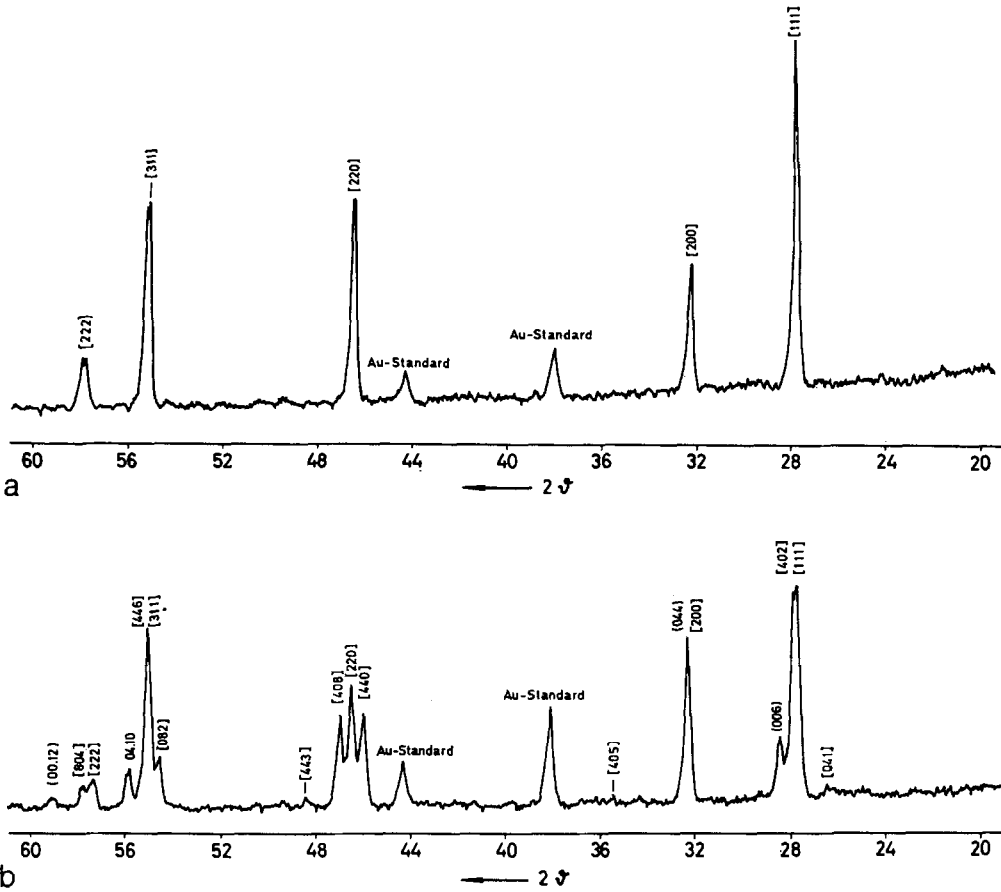


FIG. 7. X-ray spectrometer diagrams of $\text{La}_{0.50}\text{U}_{0.50}\text{O}_{2.00}$ ($T = 25^\circ\text{C}$); (a) quenched sample, prepared at 1250°C ; (b) quenched sample, prepared at 1000°C .

mens. The total entropy change Δs is given by

$$\Delta s = \Delta s_{\text{configuration}} + \Delta s_{\text{vibration}} + \Delta s_{\text{gas phase}} \quad (3)$$

The entropy of solution of oxygen per molecule is

$$\Delta S_i = \frac{\partial \Delta s(N_{\text{O}''}, N_{|\text{e}|'})}{\partial N_{\text{O}_2}} \quad (4)$$

Thus

$$\Delta S_i = \frac{\partial \Delta s}{\partial N_{\text{O}''}} \left(\frac{\partial N_{\text{O}''}}{\partial N_{\text{O}_2}} \right)_{\text{Re}} + \frac{\partial \Delta s}{\partial N_{|\text{e}|'}} \left(\frac{\partial N_{|\text{e}|'}}{\partial N_{\text{O}_2}} \right)_{\text{Re}} \quad (5)$$

where Re gives the reaction condition:

$$dN_{\text{O}_2} : dN_{\text{O}''} : dN_{|\text{e}|'} = 1 : (-2) : 4. \quad (6)$$

The basic Eq. (2) gives

$$\frac{\partial \Delta s}{\partial N_{|\text{e}|'}} = \frac{\partial \Delta s}{\partial N_{\text{U}|U|'}} - \frac{\partial \Delta s}{\partial N_{\text{U}|U|''}} \quad (7)$$

According to Eq. (6) it can be stated that

$$\left(\frac{\partial N_{\text{O}''}}{\partial N_{\text{O}_2}} \right)_{\text{Re}} = -2 \quad \text{and} \quad \left(\frac{\partial N_{|\text{e}|'}}{\partial N_{\text{O}_2}} \right)_{\text{Re}} = +4.$$

Thus Eq. (5) may be rewritten

$$\Delta S_i = -2 \frac{\partial \Delta s}{\partial N_{\text{O}''}} - 4 \frac{\partial \Delta s}{\partial N_{\text{U}|U|''}} + 4 \frac{\partial \Delta s}{\partial N_{\text{U}|U|'}}.$$

Differentiating the total entropy change Δs (Eq. 3) with respect to $N_{\text{O}''}$, $N_{\text{U}|U|'}$ and $N_{\text{U}|U|''}$, we are only considering the change of the configurational entropy, which is given by the Boltzmann equation: $\Delta s_{\text{configuration}} = k \ln$

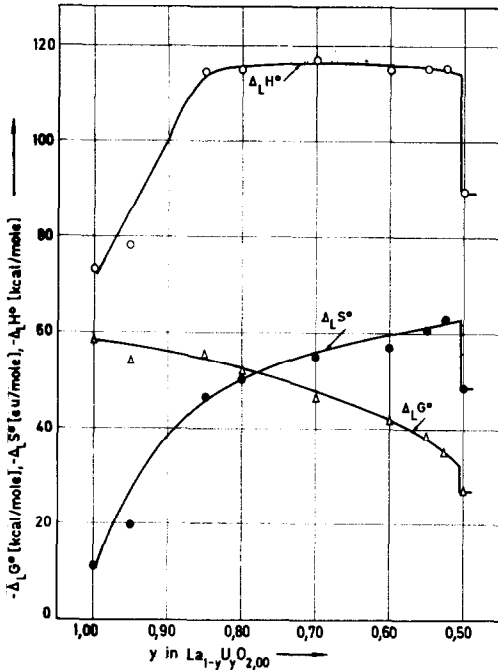


FIG. 8. $\Delta_L G^\circ$, $\Delta_L H^\circ$ and $\Delta_L S^\circ$ of the specimens $La_{1-y}U_yO_{2.00}$ as a function of y ($0.50 \leq y \leq 1$) $T = 1000^\circ C$.

$W_{O''} + k \ln W_c$. In this latter equation $W_{O''}$ is the total number of possibilities of arranging oxygen ions in interstitial positions and W_c the total number of possibilities of arranging the cations in the cationic positions.

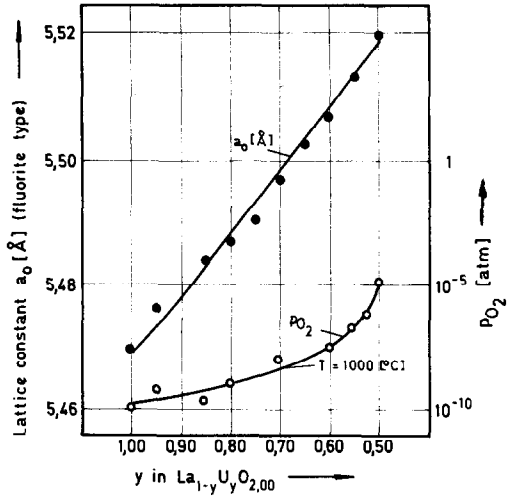


FIG. 9. Lattice constant and oxygen pressure (p_{O_2}) of the specimens $La_{1-y}U_yO_{2.00}$ as a function of y ($0.50 \leq y \leq 1$).

Also the Stirling approximation can be used in the form: $\ln N! = N \ln N - N$. Multiplication by the Avogadro number L then gives the molar entropy of solution of oxygen in the fluorite phase of $M_{1-y}U_yO_{2+x}$

$$\begin{aligned} \Delta S_{\text{calculated}} &= \Delta S_i L \\ &= 2R \left(\ln \frac{x}{1-x} + 4 \ln \frac{2x}{y-2x} \right). \end{aligned}$$

This equation differs from Aronson's formula

TABLE I

CALCULATION OF THE VIBRATIONAL ENTROPY COMPONENT $\Delta S_{\text{vibrational}}$ OF INTERSTITIAL OXYGEN FOR SOME COMPOSITIONS $M_{1-y}U_yO_{2+x}$ ($T = 1273^\circ K$)

Composition	$\Delta_L S_{\text{experimental}}$ [cal/g mole]	Reference	$\Delta S_{\text{vibrational}}$ [cal/g mole]
$La_{0.05}U_{0.95}O_{2.23}$	-48.7		17.1
$La_{0.15}U_{0.85}O_{2.23}$	-41.0		21.1
$La_{0.20}U_{0.80}O_{2.33}$	-41.0		18.9
$La_{0.30}U_{0.70}O_{2.33}$	-49.1		5.3
$La_{0.50}U_{0.50}O_{2.06}$	-68.6		20.6
$Zr_{0.10}U_{0.90}O_{2.165}$	-44.0	(18)	31.1
$Zr_{0.20}U_{0.80}O_{2.165}$	-54.0	(18)	18.0
$Zr_{0.30}U_{0.70}O_{2.165}$	-55.0	(18)	13.2
$Th_{0.29}U_{0.71}O_{2.154}$	-35.0	(17)	35.9
$Th_{0.48}U_{0.52}O_{2.122}$	-35.0	(17)	34.7
$Th_{0.71}U_{0.29}O_{2.073}$	-34.0	(17)	35.8

due to the differentiation term $\partial \Delta s / \partial N_{U|U}^{5*}$. Hence,

$$\Delta_L S_{\text{experimental}} = \Delta S_{\text{calculated}} + \Delta S_{\text{vibrational}} + \Delta S_{\text{gas phase}}$$

and $\Delta S_{\text{gas phase}}$ has the value of 60[cal/mole deg] at 1000°C (19).

Thus, the vibrational entropy component of the interstitial oxygen in the fluorite phase of $M_{1-y}U_yO_{2+x}$ can be calculated (Table I). In comparison with the values in Table I, the calculation of the vibrational entropy of excess oxygen on the basis of the development of a generalized partition function (15) gives a value of 9.4[cal/mole deg] for $UO_{2.2}$ at $T = 1600^\circ\text{K}$.

Acknowledgment

Thanks are due to the Studienstiftung des deutschen Volkes, Fonds der Chemischen Industrie and the Deutsche Forschungsgemeinschaft for financial support.

References

1. F. HUND AND U. PEETZ, *Z. Anorg. Allg. Chem.* **271**, 6 (1952).
2. D. C. HILL, J. H. HANDWERK, AND R. J. BEALS, *Report ANL-6711* (1963).
3. W. B. WILSON, C. A. ALEXANDER, AND A. F. GERDS, *J. Inorg. Nucl. Chem.* **20**, 242 (1961).
4. E. A. AITKEN, S. F. BARTRAM, AND E. F. JUENKE, *Inorg. Chem.* **3**, 949 (1964).
5. G. G. KOSCEEV, L. M. KOVBA, AND V. J. SPICYN, *Dokl. Akad. Nauk. SSSR* **175**, 92 (1967).
6. W. RÜDORFF, H. ERFURTH, AND S. KEMMLER-SACK, *Z. Anorg. Allg. Chem.* **354**, 273 (1967).
7. E. STADLBAUER, Dissertation, Universität Karlsruhe 1972, Bericht des Kernforschungszentrums Karlsruhe KFK 1649, Juli 1972.
8. H. G. DIEHL AND C. KELLER, *J. Solid State Chem.* **3**, 621 (1971).
9. K. KIUKKOLA AND C. WAGNER, *J. Electrochem. Soc.* **104**, 308 (1957).
10. K. KIUKKOLA AND C. WAGNER, *J. Electrochem. Soc.* **104**, 379 (1957).
11. U. LOTT, H. RICKERT, AND C. KELLER, *J. Inorg. Nucl. Chem.* **31**, 3427 (1969).
12. K. KIUKKOLA, *Acta Chem. Scand.* **16**, 327 (1962).
13. L. E. I. ROBERTS AND A. I. WALTER, *J. Inorg. Nucl. Chem.* **22**, 213 (1961).
14. R. PAUL, Dissertation, Universität Karlsruhe 1970, Bericht des Kernforschungszentrums Karlsruhe KFK 1297, Oktober 1970.
15. M. ATLAS, *J. Phys. Chem. Solids* **29**, 1349 (1967).
16. J. S. ANDERSON, *Proc. Roy. Soc. A.* **185**, 69 (1945).
17. S. ARONSON AND J. C. CLAYTON, *J. Chem. Phys.* **32**, 749 (1960).
18. S. ARONSON AND J. C. CLAYTON, *J. Chem. Phys.* **35**, 1055 (1961).
19. ULICH JOST, *Kurzes Lehrbuch der physikalischen Chemie*, D. Steinkopff Verlag, Darmstadt (1966).